Supplement of The Cryosphere, 18, 1215–1239, 2024
https://doi.org/10.5194/tc-18-1215-2024-supplement

The Cryosphere Open Access EGU

Supplement of

Understanding the influence of ocean waves on Arctic sea ice simulation: a modeling study with an atmosphere–ocean–wave–sea ice coupled model

Chao-Yuan Yang et al.

Correspondence to: Chao-Yuan Yang (yangchaoyuan@sml-zhuhai.cn) and Jiping Liu (liujp63@mail.sysu.edu.cn)

Table S1 The seasonal maximum and minimum simulated sea ice area (10^6 km^2) for all experiments.

Year	Exp-CFSD	Exp-PFSD	Exp-LatMelt-C	Exp-LatMelt-P	Exp-WaveFrac-P	Exp-WaveAtt-C	Exp-WaveAtt-P
2016	12.03	12.36	12.42	12.26	12.39	12.23	12.40
	3.88	3.02	3.75	3.55	3.83	3.90	3.55
2017	12.62	12.41	12.77	12.61	12.84	12.53	12.10
	3.95	3.19	4.33	4.09	3.50	4.08	3.71
2018	13.00	13.15	12.82	13.20	12.73	13.04	12.92
	3.95	3.66	4.25	3.88	3.75	3.80	3.94
2019	14.12	12.98	13.22	13.40	12.94	13.19	13.31
	4.77	4.12	4.67	4.49	4.31	4.56	4.31
2020	14.02	13.54	13.64	13.35	13.47	13.76	13.98
	4.90	3.93	4.83	4.72	4.90	4.39	4.31

Table S2 The monthly mean of the sea ice mass budget terms (top melt and basal growth), net surface heat flux at the ice surface, and the conductive heat flux for selected months of Exp-CFSD (left values of each box) / Exp-PFSD (right values of each box).

Time	Top melt (cm/day)	Basal growth (cm/day)	Net surface heat flux (W/m^2)	Conductive heat flux (W/m^2)
2016/07	-0.102 / -0.058	0.002 / 0.003	11.90 / 6.42	-1.96 / -2.95
2017/01	-0.000 / -0.000	0.421 / 0.440	-42.46 / -45.06	-42.51 / -45.12
2017/07	-0.080 / -0.085	0.002 / 0.005	4.43 / 8.27	-4.04 / -4.43
2018/01	-0.000 / -0.000	0.416 / 0.448	-44.06 / -46.09	-44.15 / -46.15
2018/07	-0.176 / -0.049	0.003 / 0.006	18.93 / 3.08	-1.71 / -3.51
2019/01	-0.000 / -0.000	0.449 / 0.454	-45.40 / -46.38	-45.43 / -46.40
2019/07	-0.027 / -0.030	0.004 / 0.007	0.09 / -1.60	-3.57 / -5.43
2020/01	-0.000 / -0.000	0.439 / 0.447	-45.38 / -51.24	-45.42 / -51.25
2020/07	-0.037 / -0.081	0.003 / 0.006	1.58 / 4.30	-3.06 / -3.63

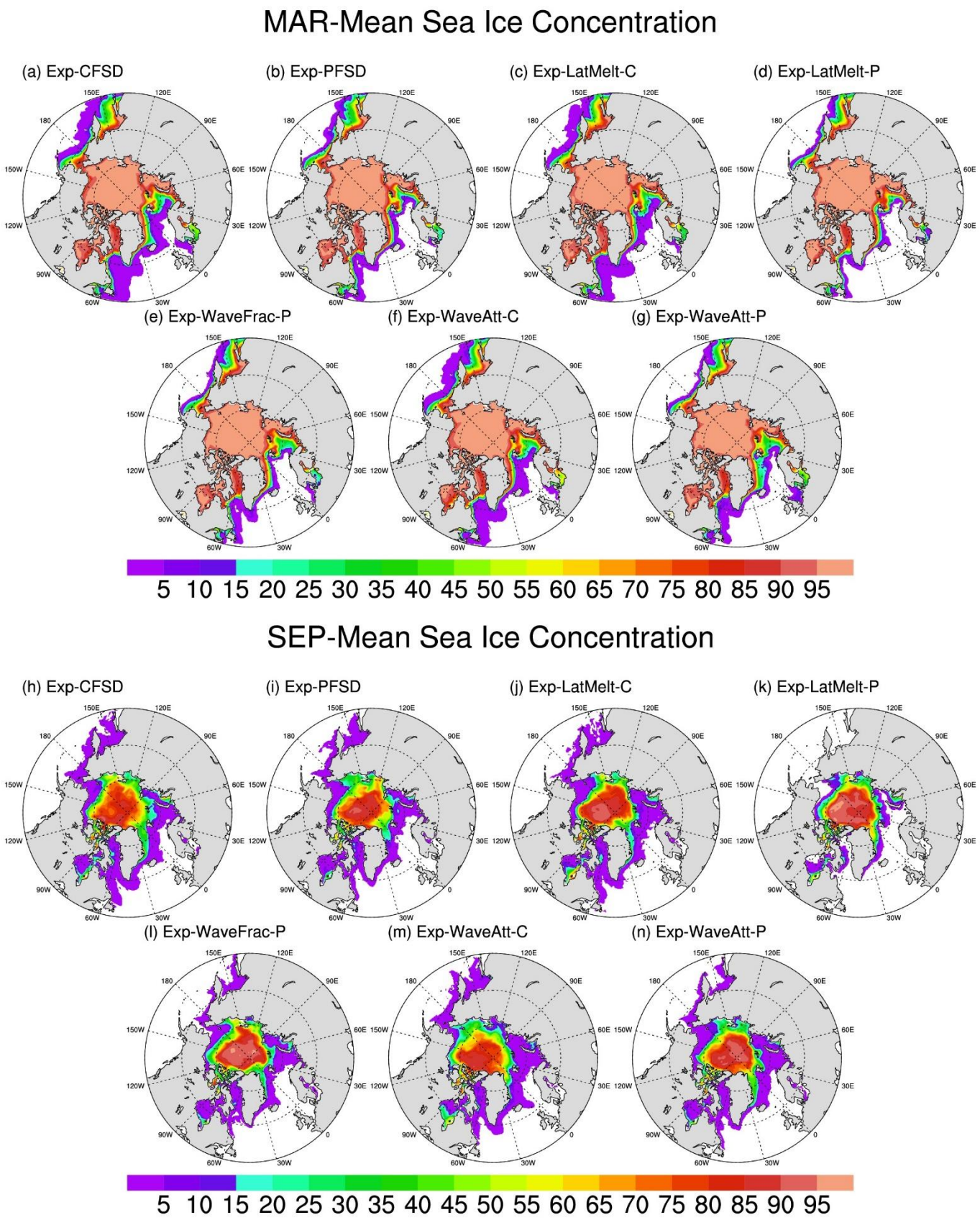

Figure S1 The (a-g) March-averagedand (h-n) September-averaged sea ice concentration during 2016-2020 for Exp-CFSD, Exp-PFSD, Exp-LatMelt-C, Exp-LatMelt-P, Exp-WaveFrac-P, Exp-WaveAtt-C, and Exp-WaveAtt-P.

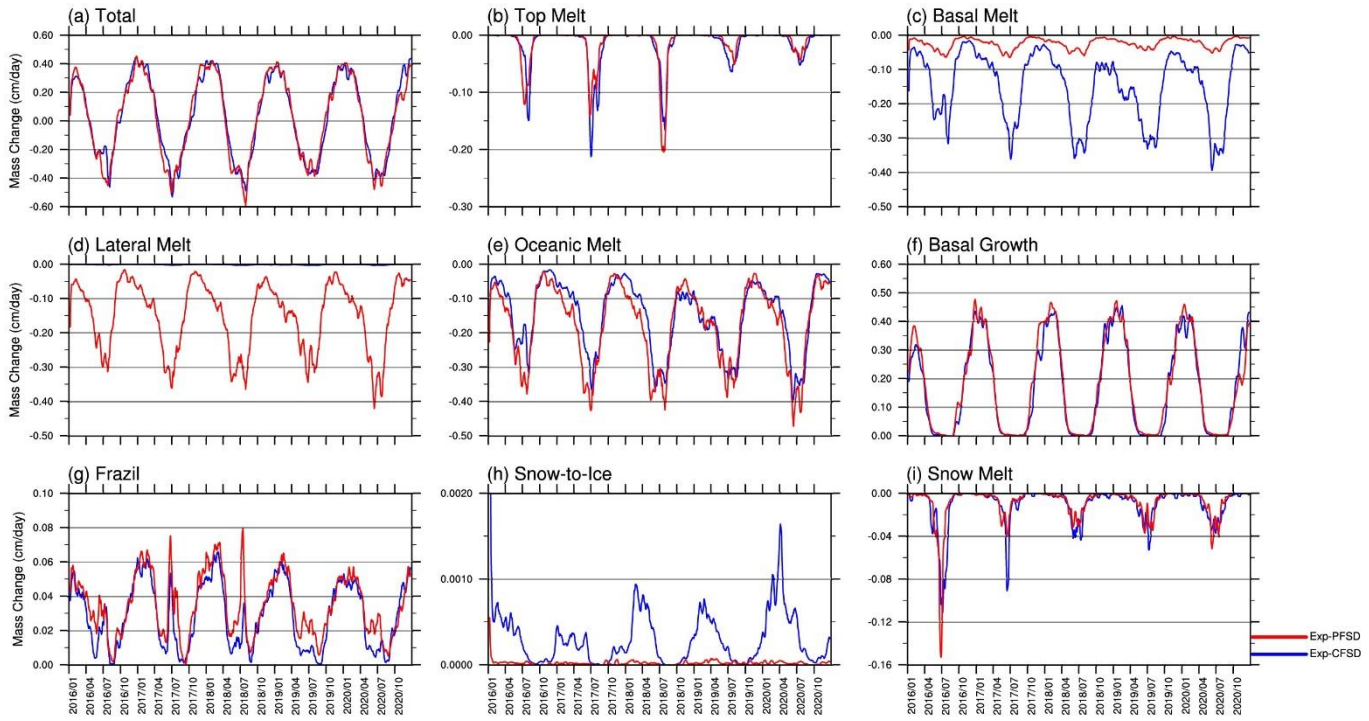

Figure S2 Time-series of (a) total mass change, (b) top melt, (c) basal melt, (d) lateral melt, (e) ice melt due to oceanic processes, (f) basal growth, (g) frazil ice formation, (h) snow to ice conversion, and (i) snow melt for Exp-CFSD (blue lines) and Exp-PFSD (red lines).

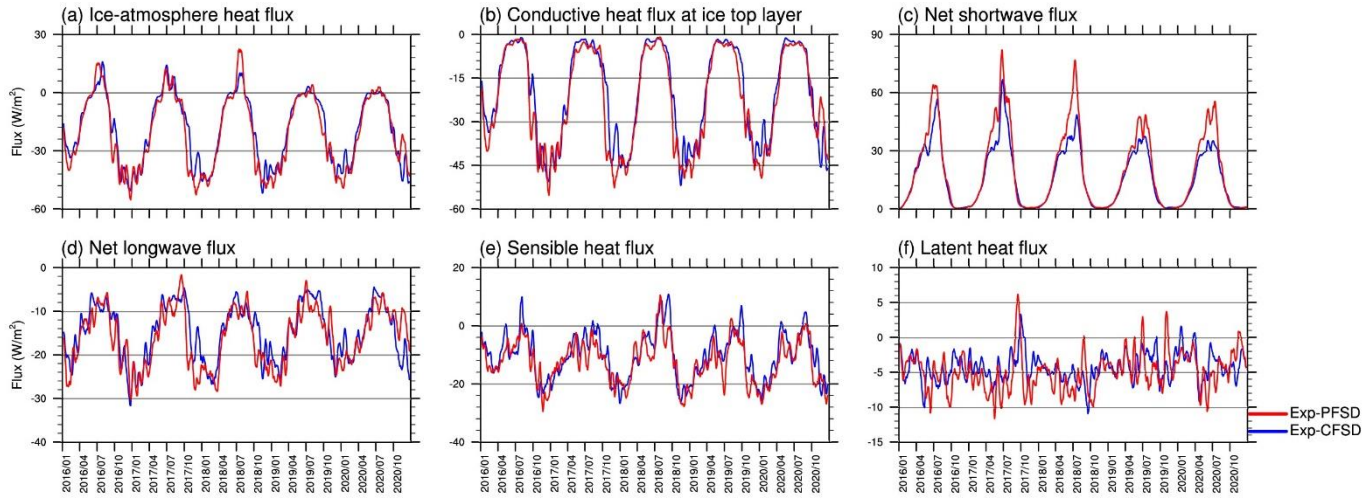

Figure S3 Same as Figure 5, but only for Exp-CFSD (blue line), and Exp-PFSD (red line).

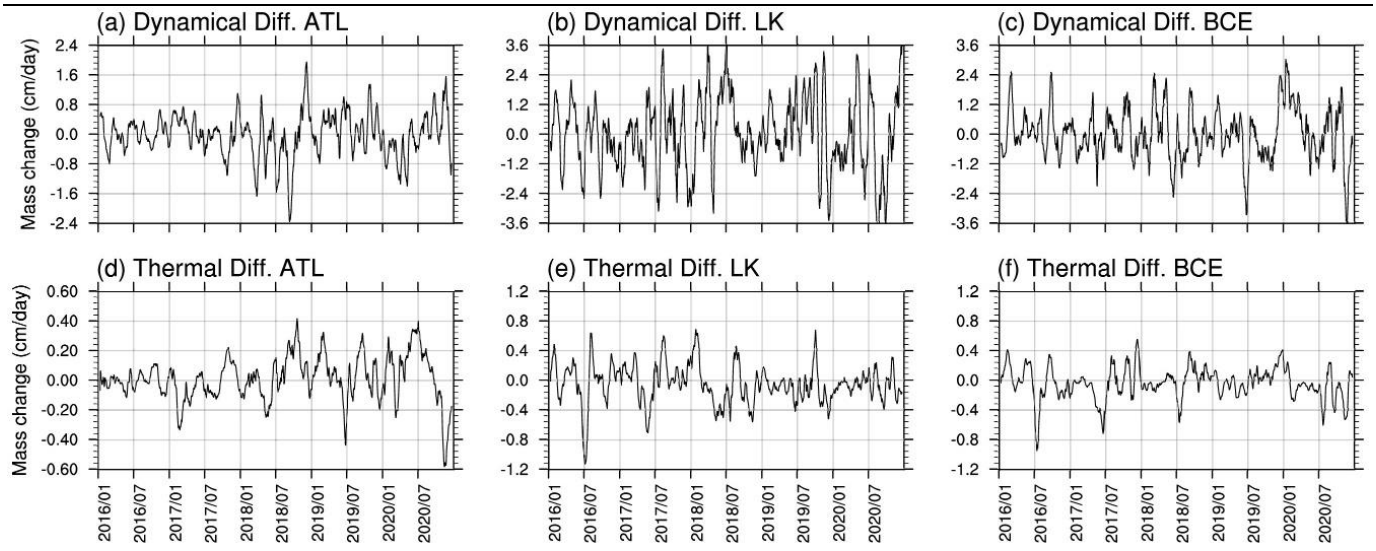

Figure S4 Time-series of the difference of (a-c) dynamical and (d-f) thermal mass change between Exp-PFSD and Exp-CFSD in the ATL, LK, and BCE regions.

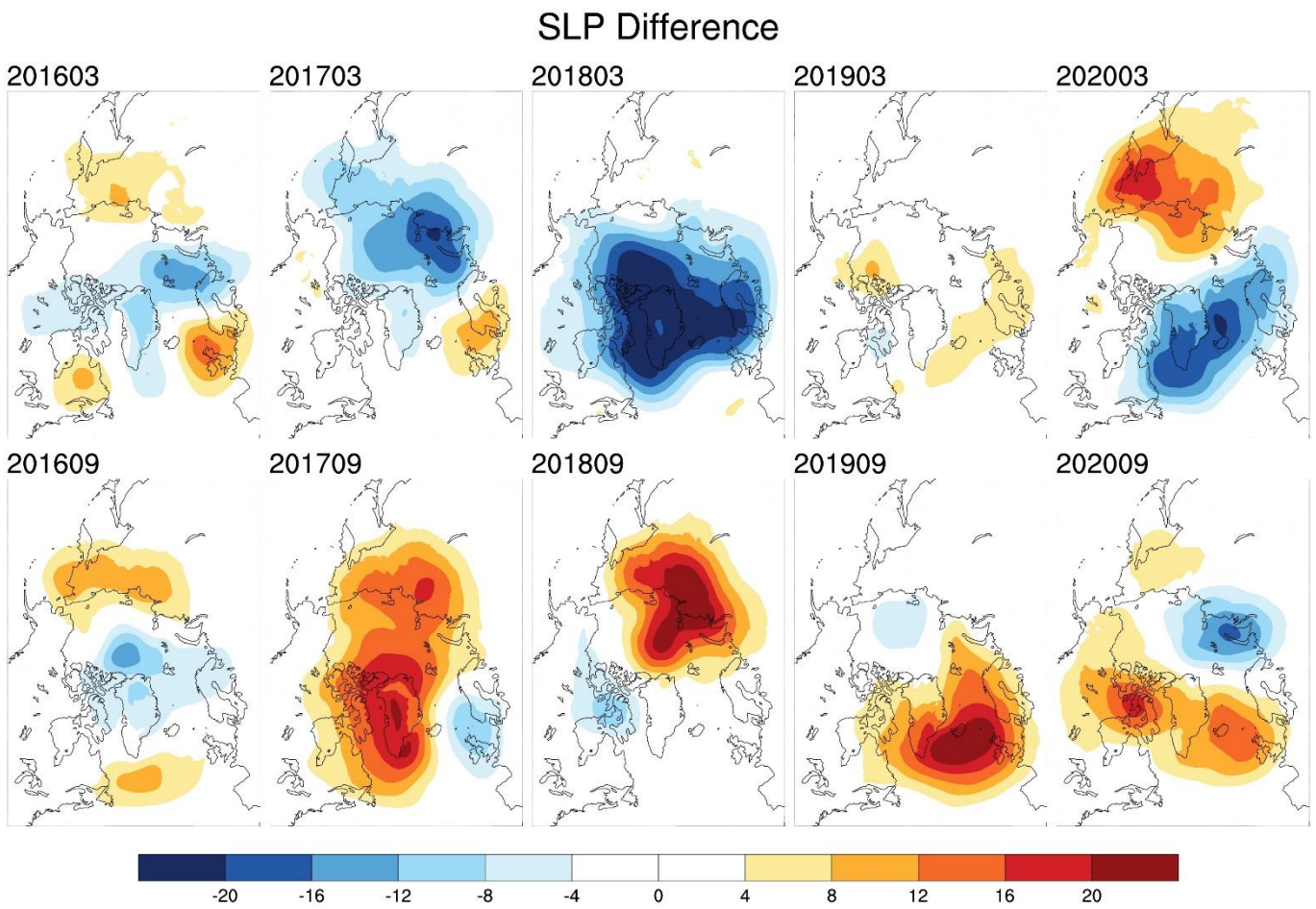

Figure S5 The difference of sea level pressure between Exp-PFSD and Exp-CFSD for March and September during 2016-2020.

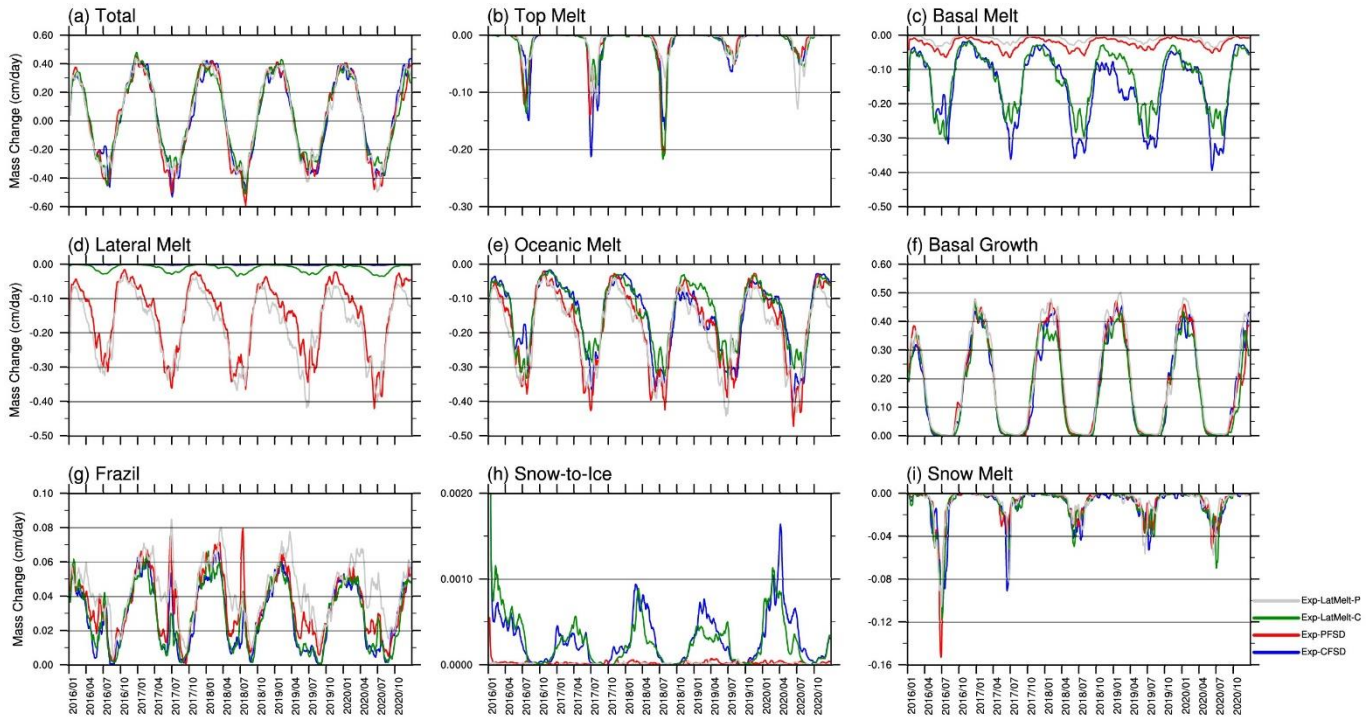

Figure S6 Same as Figure S2, but includes Exp-LatMelt-C (green lines) and Exp-LatMelt-P (grey lines).

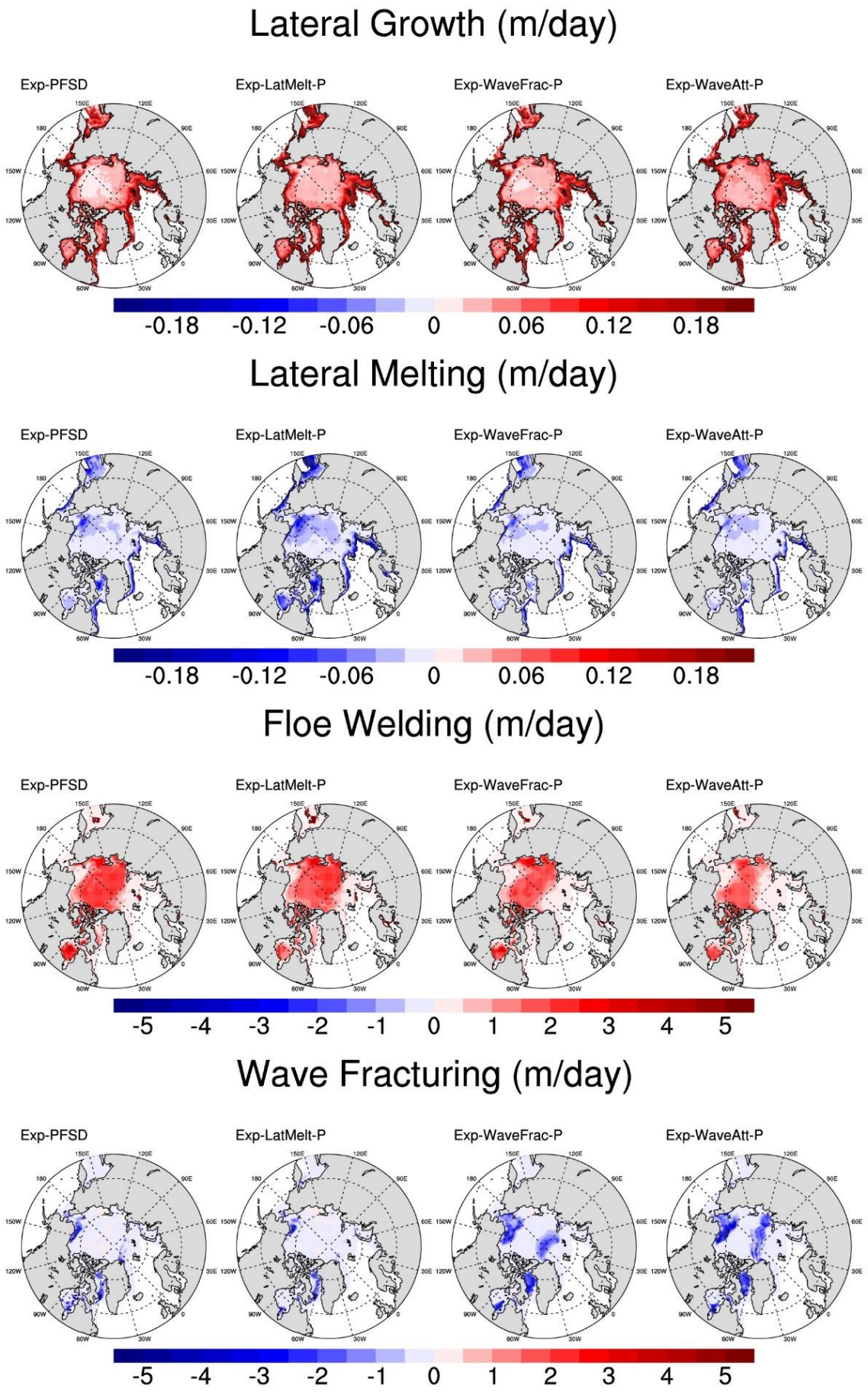

Figure S7 The tendency terms of the representative floe radius for all experiments using the prognostic FSD averaged over 01.05.2016-03.31.2016.

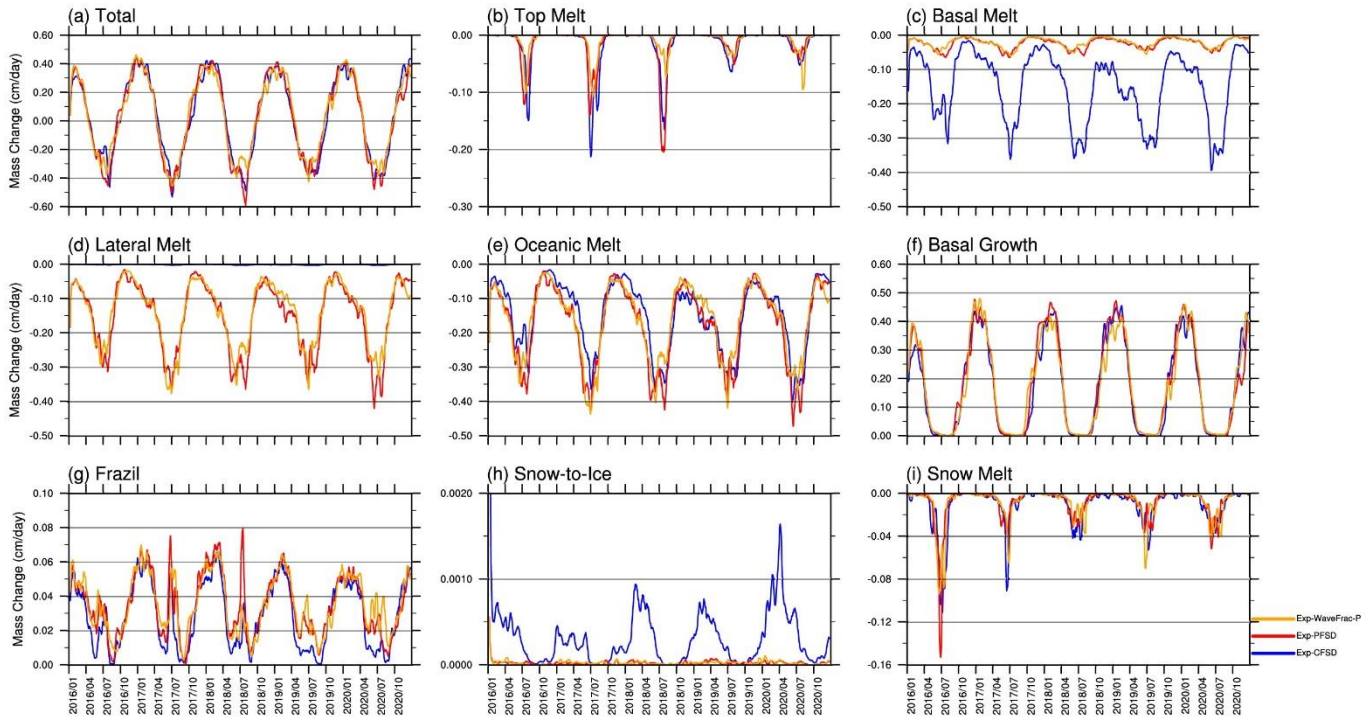

Figure S8 Same as Figure S2, but includes Exp-WaveFrac-P (orange lines).

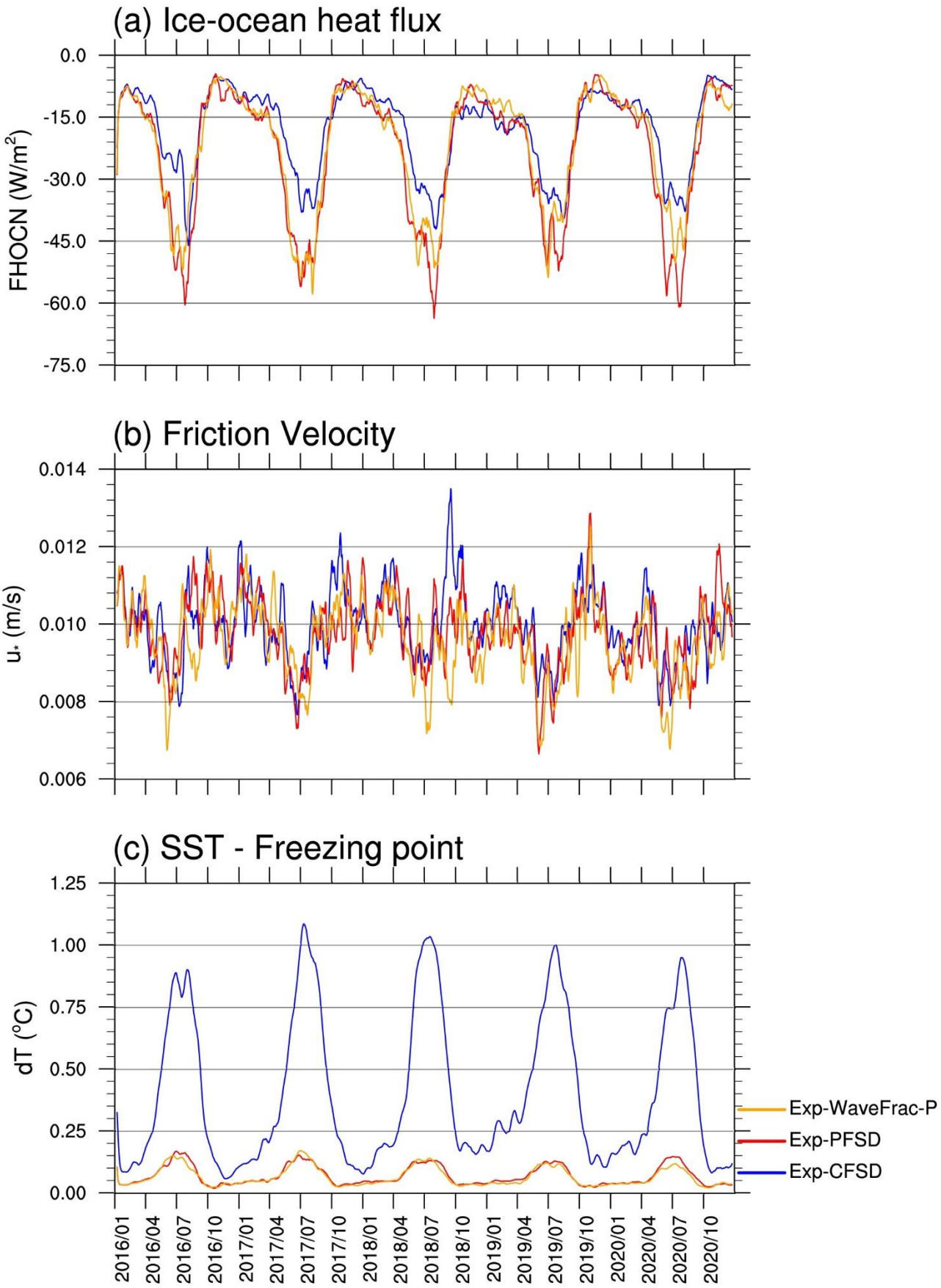

Figure S9 Same as Figure 4, but for Exp-CFSD (blue lines), Exp-PFSD (red lines), and Exp-WaveFrac-P (orange lines).

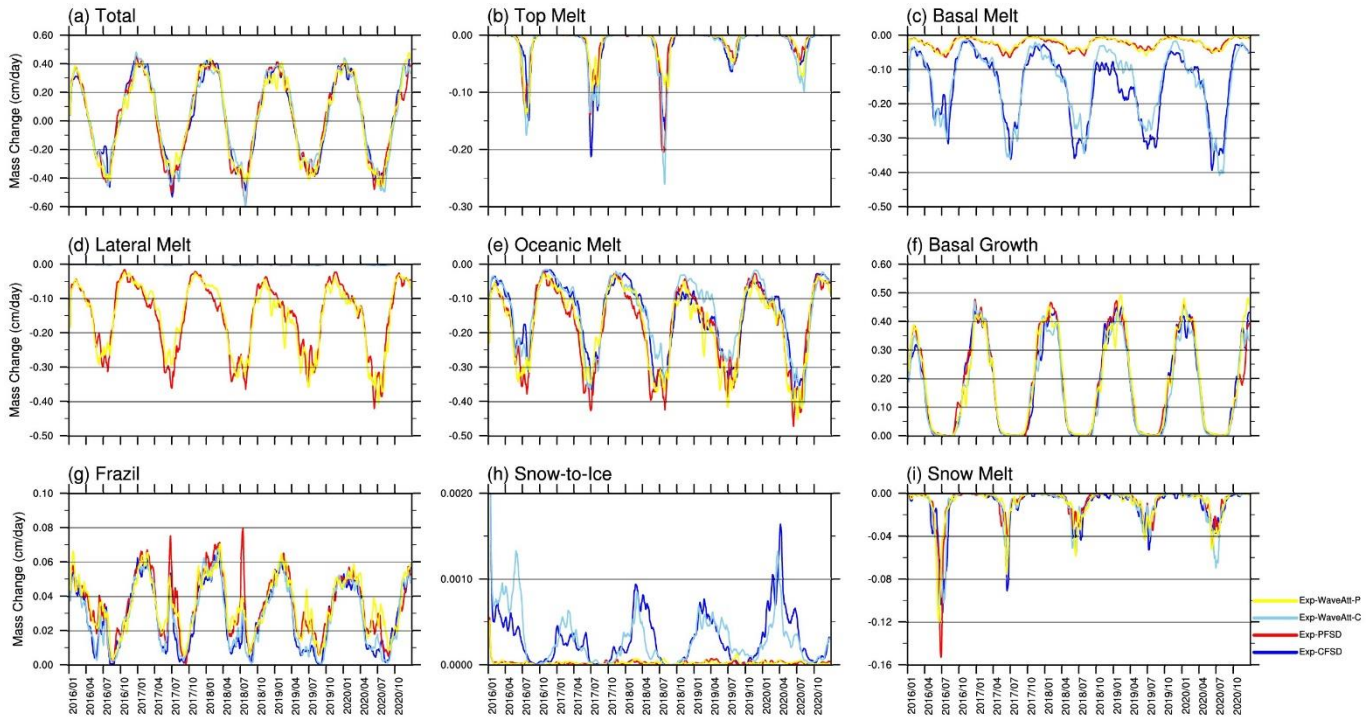

Figure S10 Same as Figure S2, but includes Exp-WaveAtt-C (light-blue lines) and Exp-WaveAtt-P (yellow lines).

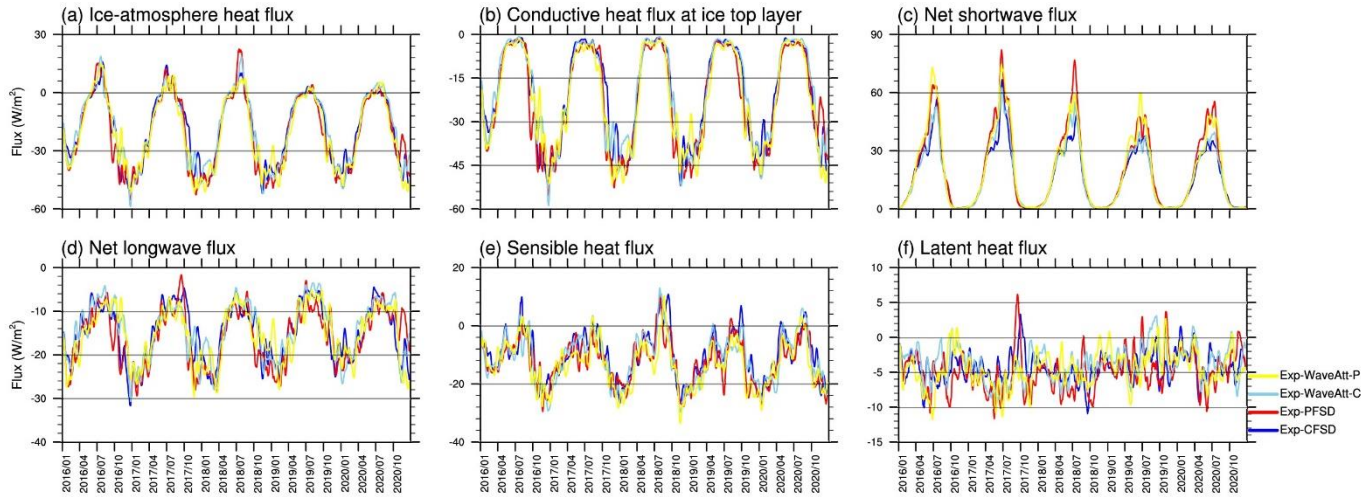

Figure S11 Same as Figure 5, but for Exp-CFSD (blue line), Exp-PFSD (red line), Exp-WaveAtt-C (light-blue line), and Exp-WaveAtt-P (yellow line).